NUREG/CR-4358
SAND85-1357
RV
Printed September 1985

# Applications of Density Profiling to Equipment Qualification Issues

K. T. Gillen, R. L. Clough, N. J. Dhooge

Prepared by
Sandia National Laboratories
Albuquerque, New Mexico 87185 and Livermore, California 94550
for the United States Department of Energy
under Contract DE-AC04-76DP00789



**Prepared for**
**U. S. NUCLEAR REGULATORY COMMISSION**

Available from

Superintendent of Documents
U.S. Government Printing Office
Post Office Box 37082
Washington, D.C. 20013-7982

and

National Technical Information Service
Springfield, VA 22161

NUREG/CR-4358
SAND85-1557
RV

# APPLICATIONS OF DENSITY PROFILING TO EQUIPMENT QUALIFICATION ISSUES

K. T. Gillen, R. L. Clough and N. J. Dhooge

September 1985

Sandia National Laboratories
Albuquerque, NM 87185
Operated by
Sandia Corporation
for the
U.S. Department of Energy

Prepared for
Electrical Engineering Instrumentation and Control Branch
Division of Engineering Technology
Office of Nuclear Regulatory Research
U.S. Nuclear Regulatory Commission
Washington, DC 20555
Under Memorandum of Understanding 40-550-75
NRC FIN No. A-1051

## ABSTRACT

This paper reviews the density profiling technique--a new, inexpensive and versatile analytical method which can yield extremely useful information on heterogeneities in polymers. The technique makes use of a density gradient column to measure the density of a series of successively-cut slices across a sample. Since the density of very thin slices can easily be obtained, density profiles across very small cross-sections (<1 mm) are readily available. A major application of the technique involves oxidation studies of polymers, since oxidation reactions usually lead to substantial increases in polymer density. Diffusion-limited oxidation effects, which lead to heterogeneously oxidized materials, are often present in polymer aging studies in air. Since these effects are responsible for the commonly-observed physical dose-rate effects in radiation aging environments and for non-Arrhenius behavior in thermal aging environments, the availability of simple oxidation profiling techniques is a tremendous aid in validating the aging simulation aspects of equipment qualification procedures. This paper gives examples of the utility of density profiling for studying oxygen diffusion-limited degradation in both radiation and thermal aging environments and in discovering/understanding chemical dose-rate effects in high energy radiation environments.

CONTENTS

LIST OF FIGURES

# EXECUTIVE SUMMARY

An important aspect of equipment qualification involves the accelerated simulation of the natural aging expected for a material or component. In various aging environments (e.g. heat, radiation), the presence of air (i.e., oxygen) can greatly complicate any attempt to interpret accelerated aging data. These complications are due to physical and chemical mechanisms, both of which must be understood in order to have confidence in any accelerated simulations. Physical effects are common in both radiation and heat-aging environments and are caused by diffusion-limited oxidation. At high radiation dose rates or high enough oven temperatures, the oxidation in a material will use up the dissolved oxygen faster than it can be replenished from the surrounding atmosphere by diffusion through the material. This leads to oxidation gradients in the material, with more oxidation near air-exposed surfaces and less in the interiors. Macroscopically, this can lead to dose-rate effects in radiation environments and non-Arrhenius effects in oven-aging studies. Interpretation of accelerated aging results can also be complicated by chemical mechanisms, whenever some chemical step in the kinetics underlying degradation occurs on a time scale comparable to the sample exposure time.

Techniques capable of monitoring and understanding such mechanisms are crucial to the development of valid accelerated aging methodologies. A new technique which achieves these goals, density profiling, is extensively reviewed in this document. This inexpensive and sensitive analytical method makes use of a density gradient column to measure the density of a series of successively-cut slices across a sample, thereby mapping any density heterogeneities. Since oxidation reactions usually lead to substantial increases in polymer density, the capability of the technique for profiling samples allows one to monitor the heterogeneities caused by such mechanisms as diffusion-limited oxidation.

Since samples to be profiled often have small cross-sections (less than 1 mm), we describe a technique involving a commercial vibrating razor blade apparatus which allows us to obtain uniform slices for elastomeric materials down to ~50 micrometers thickness. We also describe a method for easily and reliably creating density gradient columns with good linearity and predictable density ranges. Sources of possible systematic error in density measurements are described together with techniques for recognizing and minimizing these errors.

Some representative density profiling data is shown to illustrate the breadth of information available from the technique. Density profiling data is used to show that a radiation dose-rate effect for the mechanical properties of a cross-linked polyethylene

material is due to diffusion-limited oxidation effects. Density profiles of a low density polyethylene material show unambiguously that the large dose-rate effects found for its mechanical properties are due to a combination of physical and chemical dose-rate effects. For thermally-aged materials, density data are used to confirm the presence of oxygen-diffusion-limited degradation and to illustrate the power of the technique for observing inhomogeneous oxidation effects caused by localized material poisoning or incompatibilities.

# INTRODUCTION

For polymer applications in air, oxidation processes often dominate degradation. Important oxidation effects are observed in most aging environments including elevated temperature, high-energy radiation and mechanical stress. Exposures in air often lead to inhomogeneously oxidized samples, complicating attempts both to understand the oxidation processes and to extrapolate accelerated exposures to long-term, real-time, conditions. Inhomogeneous oxidation can result from either initially inhomogeneous material or incompatibility problems with neighboring materials.

Inhomogeneous oxidation can also be caused by oxygen-diffusion limited degradation. This well-known effect [1,2,3] occurs whenever the rate of oxygen consumption in the polymer is greater than the rate at which oxygen from the surrounding atmosphere can be resupplied to the interior by diffusion processes. The importance of this effect will therefore depend upon material geometry, the oxygen consumption rate and the oxygen permeation rate.

In radiation aging, the presence of diffusion-limited oxidation will lead to so-called physical dose-rate effects, which can greatly complicate accelerated aging simulations [4,5,6]. For thermal aging, these same effects can lead to non-Arrhenius behavior [7]. Therefore, being able to monitor and understand such effects is a critical need in the development of aging methodologies relevant to nuclear power plant qualification procedures.

Attempts are often made to eliminate diffusion anomalies in aging tests by studying thin samples. This approach may have several problems. First the thin sample may not be thin enough, since oxidation depths may reach only fractions of a millimeter under typically-used, laboratory-aging, conditions. Second, the properties of the specially-prepared thin sample may be unrepresentative of the bulk material, due either to different curing conditions or because aging of these laboratory samples may overlook dominant degradation effects caused by the lack of impurities introduced during processing of the real material. These impurities may be responsible for important degradation effects [4].

We have been interested in developing techniques for both monitoring heterogeneous oxidation and understanding the underlying mechanisms [4,5,6] for commercial, as well as laboratory-prepared, samples. Our goal is to develop techniques capable of mapping inhomogeneous degradation across samples with thicknesses as small as a millimeter or less. A number of previous approaches have been successfully used for certain special types of materials. When aging leads to measurable color changes, for instance, color

development can be monitored [8]. For initially uncrosslinked materials, the depth dependence of crosslinking versus scission processes has been followed using solubility measurements [9] and gel permeation chromatography [8].

This paper describes, in detail, a new technique which we refer to as density profiling. The technique depends on the observation that significant changes in density usually occur during oxidation of polymeric samples. Since the density of extremely small samples can be accurately monitored using a density gradient column, changes in density occurring over very small distances can be obtained. The technique can be applied to a large variety of materials, regardless of opacity or crosslinking. Representative data for samples aged in heat, high-energy (specifically, gamma) radiation and under mechanical-stress environments are given to show the utility of density profiling for recognizing the existence of heterogeneous oxidation, mapping the shapes of oxidation profiles and aiding both in the elucidation of the oxidation mechanisms and in the development of aging methodologies.

Two additional profiling methods, involving the optical examination of reflected light from cross sections of metallographically-polished samples and the profiling of relative hardness across these samples, are described in a separate publication [5]. These techniques yield information complementary to density profiling,

## EXPERIMENTAL

### Materials

The five materials studied were commercial formulations. Three were cable insulation materials, a chemically crosslinked polyethylene (CLPE), a noncrosslinked low density polyethylene (PE) and an ethylene propylene rubber (EPR). The other two were seal and gasket materials obtained in sheet form, an ethylene propylene rubber and a nitrile rubber.

### Aging Exposures

Heat aging and high-energy gamma irradiations were carried out in Sandia's aging facilities, which are described elsewhere [10]. Throughout aging, a steady flow of air was supplied to the sample chambers at a rate equivalent to approximately two changes of atmosphere per hour.

### Tensile Measurements

Tensile tests were performed using a Model 1130 Instron with an electrical tape extensometer clamped to the sample. Samples were strained at 12.7 cm/min with an initial jaw separation of 5.1 cm.

Elongation at break and ultimate tensile strength were measured at room temperature.

Sample Preparation

The nitrile rubber and EPR seal materials were cut from sheet material and aged as rectangular strips of approximate dimensions 0.6 cm by 15 cm. The remaining materials were cable insulations which had their copper conductors (either single or seven-stranded) removed prior to aging. Thus air (oxygen) was available during the aging both on the outside and inside (where the conductor would normally reside) of the insulation. The top part of Figure 1 shows sketches of a sheet sample and of cross sections through one- and seven-conductor insulation samples and indicates how density samples are obtained. Sectors are cut for the insulation samples so that the overall density results will represent the average insulation density.

Various methods can then be used to obtain the thin slices (~50-250 micrometers) needed for density profiling and shown in the lower part of Figure 1. The crudest method involves slicing with a hand-held razor blade. Although this method can be difficult if thin slices are required, it is usually satisfactory for thicker slices, for screening studies, and for instances where semi-quantitative profiles are sufficient. In principle, microtoming techniques should yield uniform thin slices. In practice, especially for elastomeric materials, we had difficulty achieving satisfactory results with most standard one-pass microtomes. However, by using a Lancer Vibratome Series 1000 Sectioning System, which features a vibrating razor blade, we were able to achieve excellent results even for elastomers. A schematic of the arrangement is shown in Figure 2. Overall density samples are glued (using a cyanoacrylate adhesive) to the top and approximately flush with the leading edge of a mounting block. For horizontal support during the slicing, a piece of eraser larger than the sample is first glued behind and adjacent to the intended location of the sample and the sample is then mounted flush against the eraser. The uniformity of the slices for a given material will depend on the size and stiffness of this backing material. For rubbery materials, we find that a soft art gum eraser gives good results. By utilizing a Vibratome blade angle of zero degrees (blade parallel to slicing direction), half-length razor blades, maximum back and forth blade amplitude, minimum forward speed of the clamped mounting block and water lubrication, we are able to obtain uniform slices down to thicknesses of 25 to 50 micrometers for most elastomeric materials. The best results are achieved using the thin blades obtained upon taking apart twin shaving blades available from numerous commercial manufacturers.

After slicing, a micrometer is used to assess the uniformity in thickness across each slice and to estimate its average thickness.

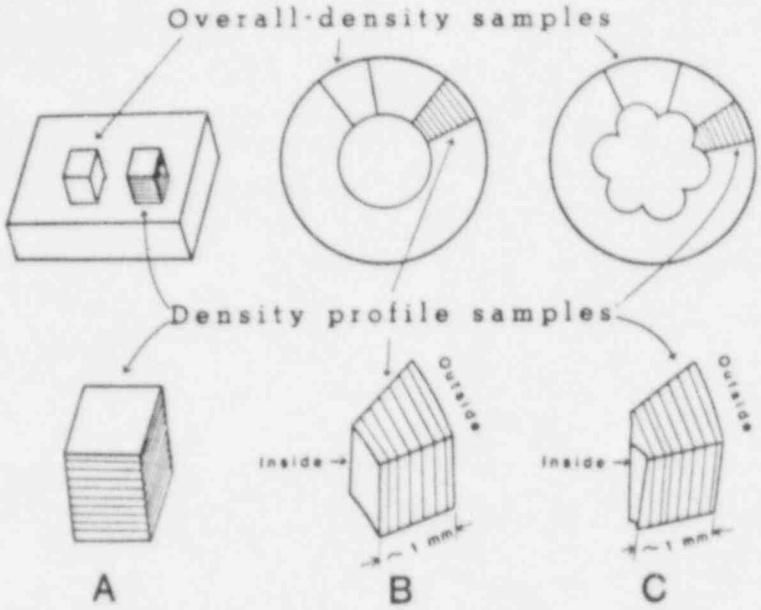


Figure 1: Schematic illustrating how overall density samples and density profile samples were obtained for three types of materials. A: sheet materials. B: single-conductor insulation samples. C: seven-conductor insulation samples.

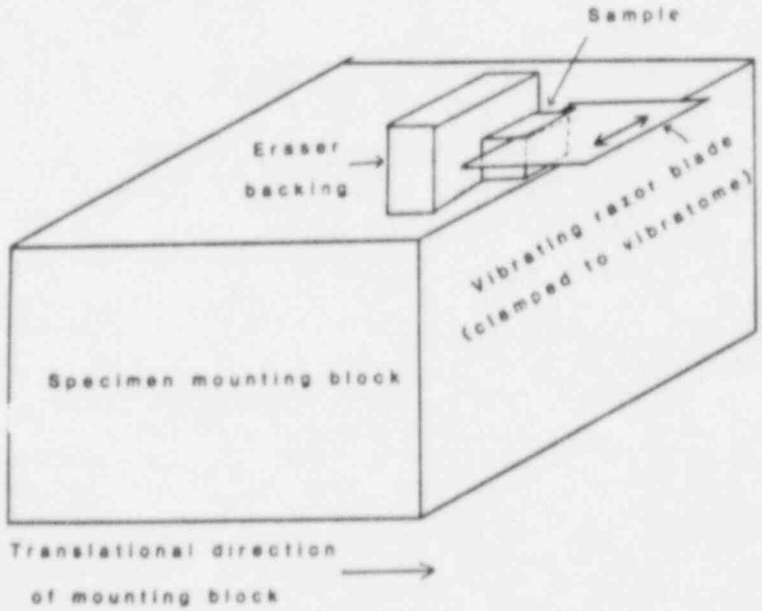


Figure 2: Schematic representation of the experimental arrangement used to obtain density profile samples using the Lancer Vibratome Sectioning System.

For data presentation, we take the overall sample thickness to be the summation of the estimated average thicknesses of its slices. This allows us to calculate the relative positioning of each slice with respect to the material's cross section. For a profile of a sheet material, the relative positioning of slices is defined quantitatively but the situation becomes less quantitative for more complicated cross sections, such as near the inside surface of the insulation material removed from seven-stranded conductors.

Density Column Procedures

The normal procedure for creating a density column involves gravity-fed mixing of high and low density liquids. Since we had difficulty creating linear columns with predictable density ranges utilizing such techniques, we used a modified mixing procedure based on liquid pumps, shown schematically in Figure 3. The flasks marked A and C contain (respectively) the high and low density liquids which are mixed to create the gradient column. B and E are Cole Parmer Masterflex Peristaltic pumps (Model nos. 7543-06 and 7543-12 respectively), chosen so that the liquid pumping rate of E (~500 cc/h using 3 mm inside diameter tygon tubing) is twice that of B. The output of B is dripped into flask C; efficient mixing is achieved using a magnetic stirrer, D. A capillary tube, H, connected to the output of pump E, extends to the bottom of the gradient tube, G, and is used to fill the column. Assuming the pumping rate of B is half that of E, the initial volume of low density liquid in flask C is chosen to be half the volume of the gradient tube, G. This will ensure that flask C will be approximately empty when G is filled and therefore that the density at the bottom of the completed column will approach the density in flask A. The initial volume in flask A is unimportant so long as sufficient volume exists to guarantee that there is some liquid remaining when the gradient tube is filled. For our case, using a volume which is greater than ~60% of G will assure this. After the gradient tube is filled, valve F is closed and the capillary tube is carefully removed. We find that this arrangement gives columns with good linearity and predictable density ranges.

Our gradient columns (available from SGA Scientific Inc.) are of concentric double wall construction, allowing temperature control with a circulating bath set at 23°C. The columns are calibrated using glass calibration balls of known density (measured at 23°C) which were obtained from Techne, Inc. Typical column resolution is 0.002 g/cc per centimeter of column height.

For measurements above 1.0 g/cc, columns were made using calcium nitrate-water solutions; below 1.0 g/cc, water-ethanol solutions were used. Many factors need to be considered when choosing the liquids for a column. Our primary criterion was avoiding selective absorption problems [11,12], where substantial density errors can

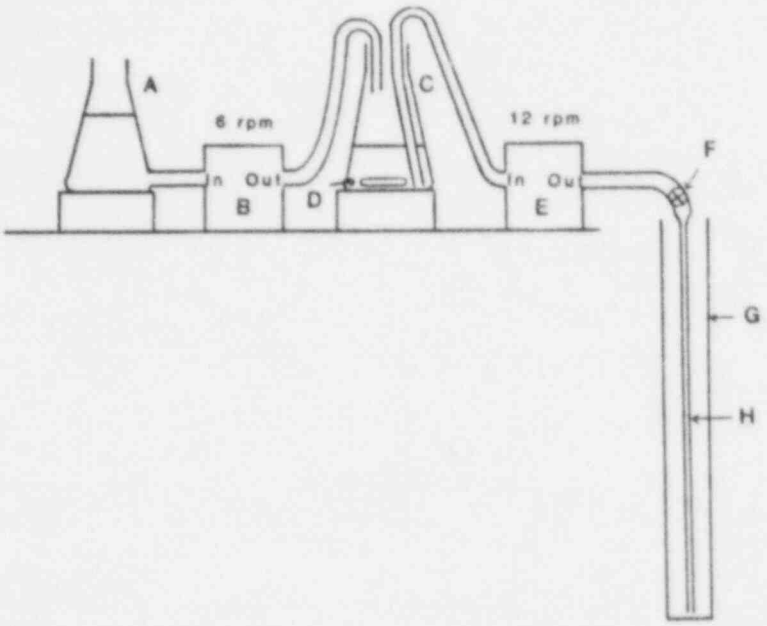


Figure 3: Schematic of the experimental setup used to prepare density gradient columns. A and C are flasks that contain the high density and low density solutions, respectively. B and E are liquid pumps chosen such that the pumping rate of E is approximately twice that of B. D is a magnetic stirrer used to assure efficient mixing of the two solutions. H is a capillary tube used to fill the gradient tube, G.

result. For polyolefin materials, this problem is usually insignificant in columns containing water and ethanol due to their limited solubilities (typically less than 0.05% by volume). Most other candidate organic liquids, such as p-xylene, $CCl_4$, toluene and chlorobenzene, have orders of magnitude larger solubilities and can therefore yield large selective absorption errors. We are also concerned with changes in density caused by oxidation and, since oxidation can effect selectivity, this is a further reason to avoid such columns. Another advantage of using columns made from ethanol and water is the lack of toxicity concerns.

The possibility that the large interfacial tension gradient between ethanol and water could cause density errors in ethanol-water columns has been addressed in two careful studies [11,12], both of which concluded that such effects are not significant. To confirm these conclusions, we compared some of our ethanol-water density results with measurements taken in alternative organic mixtures having small interfacial tension gradients and observed no significant differences. For instance the density of the unaged

polyethylene material was measured as 0.925±0.002 g/cc in ethanol-water (after 15 minutes, with no change 3 days later) and 0.923±0.002 g/cc in toluene-chlorobenzene (after 15 minutes). Because of the selective sorption of toluene, however, the latter result slowly dropped to 0.919±0.002 g/cc after 3 days.

Since air bubbles attached to samples will result in density values which are lower than actual, proper wetting of samples prior to introduction into the column is another concern. Using a microscope, the surfaces of the samples can be examined for air bubbles after placement in the bottom of a shallow glass dish containing a solution of density lower than the sample. In instances where air bubbles are a problem, the sample can be wetted after pumping on a vacuum system. A second approach, which we have found to be useful for certain materials, involves improving their wettability by treating them for a few minutes with an argon plasma. A 4000 Series plasma chamber manufactured by Branson International Plasma Corporation is used with flowing argon gas at a power level of 50 watts. Samples are exposed for 3 minutes, turned over and exposed for an additional 3 minutes. Another possible approach, which we have not attempted, involves the use of surfactants.

Density Measurements

After introduction into the top of a density gradient column, the sample falls until it reaches the point at which the liquid density in the column equals the sample density. The time to reach this position depends on sample shape and size and on the gradient fluid viscosity. Large samples (~1 $mm^3$) reach "equilibrium" in a few minutes whereas small samples may require many hours. The positions of the glass density standards are recorded and used to make a column calibration curve which allows the sample density to be calculated.

Some simple observations and experiments can be used to eliminate any remaining concerns over the possible presence of small air bubbles not observed with the microscope and artifacts caused by selective absorption of a column liquid. When materials selectively absorb liquid of density lower than the sample (e.g., water from a salt water column), the sample will first sink to a minimum in the column and then start floating upward as the absorption continues to swell the material. It could be argued that during the long times required (hours) for small samples to reach "equilibrium" in the column, this sorption process may achieve equilibrium. Thus a minimum followed by a rise in the column might not be observed even in the presence of significant swelling. Large samples, however, approach equilibrium density conditions within minutes, a time much less than it takes for sorption equilibrium, given the larger sample dimensions coupled with the smaller time. If selective sorption of the less dense liquid occurs for these samples, they will then slowly rise (or

fall if higher density fluid selectivity absorbs) over a much longer time scale [11]. Thus, concerns about selective sorption effects are eliminated in screening experiments where overall density samples (Figure 1) of varying size are observed in the column. If these screening tests show that the equilibrium density is independent of sample size, concerns about microscopic air bubbles are also eliminated, since the surface-to-volume ratio increases significantly as the sample size decreases. A second and similar check for possible artifacts such as small bubbles involves comparison of the overall-sample density with the weighted average density of the slices used for profiling the sample. It should also be mentioned that the importance of sorption can change as a material becomes oxidized, implying that these effects may appear for aged materials even if they are minimal for unaged materials.

For the materials and aging conditions studied in this paper sorption problems were found to be minimal. This result is expected for the polyolefin materials, since water and alcohol sorption is typically small. We did observe water sorption effects for a plasticized PVC and for a chloroprene rubber, making interpretation of density data more difficult. For these materials, a column made from different liquids might be more useful.

## RESULTS AND DISCUSSION

### Representative Results for Radiation-Aged Materials

The aging mechanisms underlying degradation of polymeric materials in high energy radiation environments can be quite complex [4,5,6]. In the presence of air (oxygen), radiation dose-rate effects and synergisms of radiation and temperature are often observed. These effects, which must be understood to make confident predictions about material responses, can be divided into two types, physical and chemical. Physical dose-rate effects are common during radiation exposures and are caused by diffusion-limited oxidation. At high dose rates, dissolved oxygen is used up faster than it can be replenished from the surrounding atmosphere, resulting in more oxidation near air-exposed surfaces and less in the interior. As the dose rate is lowered, the oxidation will proceed further into the sample, leading eventually to a homogeneously-oxidized material. Chemical dose-rate effects occur whenever some process in the rate kinetics underlying degradation occurs on a time scale comparable to the sample exposure time.

We will show that density profiling is very useful for elucidating these mechanisms by describing some results for the crosslinked polyethylene (CLPE) and the low density polyethylene. Figure 4 shows mechanical property data for the CLPE material aged at 43°C in our Cobalt-60 radiation aging facility [10]. The ultimate

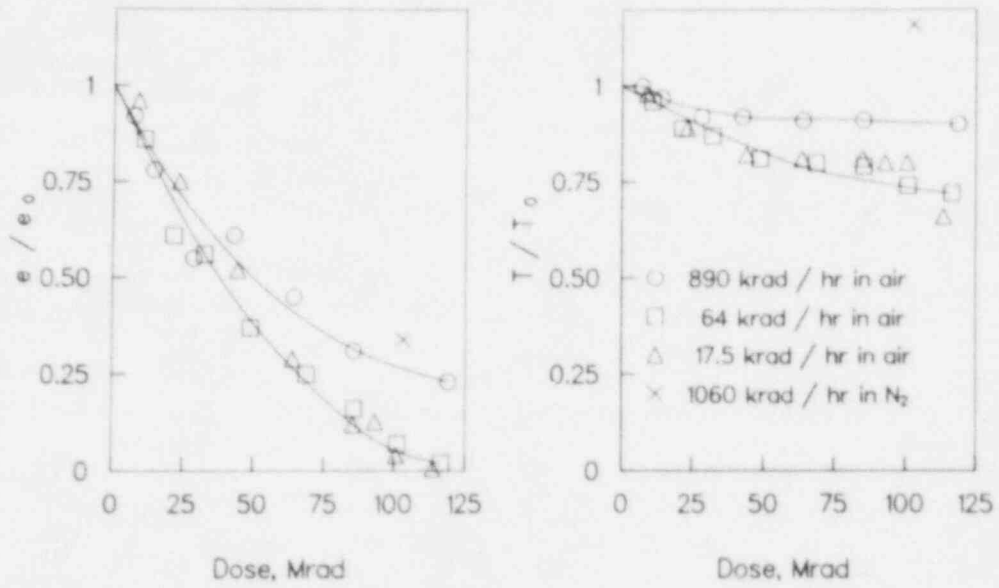


Figure 4: Mechanical property results for the radiation aging of a chemically crosslinked polyethylene cable insulation material at 43°C. The tensile strength after aging divided by the tensile strength before aging ($T/T_o$) and the tensile elongation after aging divided by the tensile elongation before aging ($e/e_o$) are plotted against the total integrated radiation dose under the various indicated dose-rate and atmospheric conditions.

tensile elongation, e, and the ultimate tensile strength, T, divided by their unaged values, $e_o$ and $T_o$, are plotted against the integrated radiation dose at the indicated dose rates. Exposures were carried out under conditions of slow air flow, except for the points labeled with an "x", which refer to exposures in a nitrogen atmosphere. Comparing the nitrogen and air aging results clearly shows that oxidation mechanisms are important for the degradation. In air environments, the mechanical deterioration appears to be sensitive to dose rate somewhere above 70 krad/h, but appears to be independent of dose rate below this level.

Overall density results for this material are shown in Figure 5. Note first the very slight increase in density as a function of total dose for the sample aged in nitrogen. Many materials aged in nitrogen have similar small increases in density. Since weight increases are impossible in a nitrogen atmosphere, these results imply slight shrinkages in these materials, probably as a result of crosslinking caused by the radiation. The samples irradiated in air, on the other hand, show large increases in density. In air environments, the sample weight will increase due to reactions

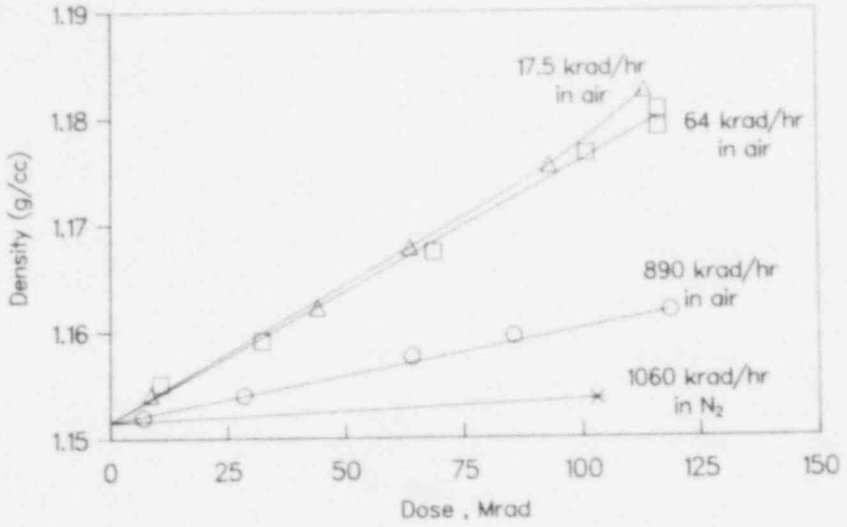


Figure 5: Overall density results for the chemically crosslinked polyethylene cable insulation material. Density is plotted versus total radiation dose under the various indicated experimental conditions.

which covalently bind oxygen, but decrease due to formation of gaseous products such as $H_2$, $CO_2$, CO and $CH_4$. For radiation exposures at low to moderate temperatures in the presence of air, sample weights are usually found to increase, implying that the first mechanism dominates. Since this increase in weight is usually smaller than the density increase, overall shrinkage must occur in the material. The fact that the observed density increases are due to a combination of a weight increase coupled with a volume decrease is one major reason for the striking sensitivity of the overall density to the relatively subtle dose-rate effects noted for the mechanical properties.

In the air environments, the effect of dose rate on the overall density results for CLPE (Figure 5) show excellent correlation to the mechanical property results of Figure 4. Note also that the overall density data is approximately linear with dose. This linearity implies that the reactions responsible for the degradation are not time dependent; in other words, the oxidation is not autocatalytic. Reaching a similar conclusion from data less directly related to the chemical reactions (e.g., mechanical property data) would be difficult.

Results from density profiling are even more instructive than those from overall density. Figure 6 shows density profiles for unaged

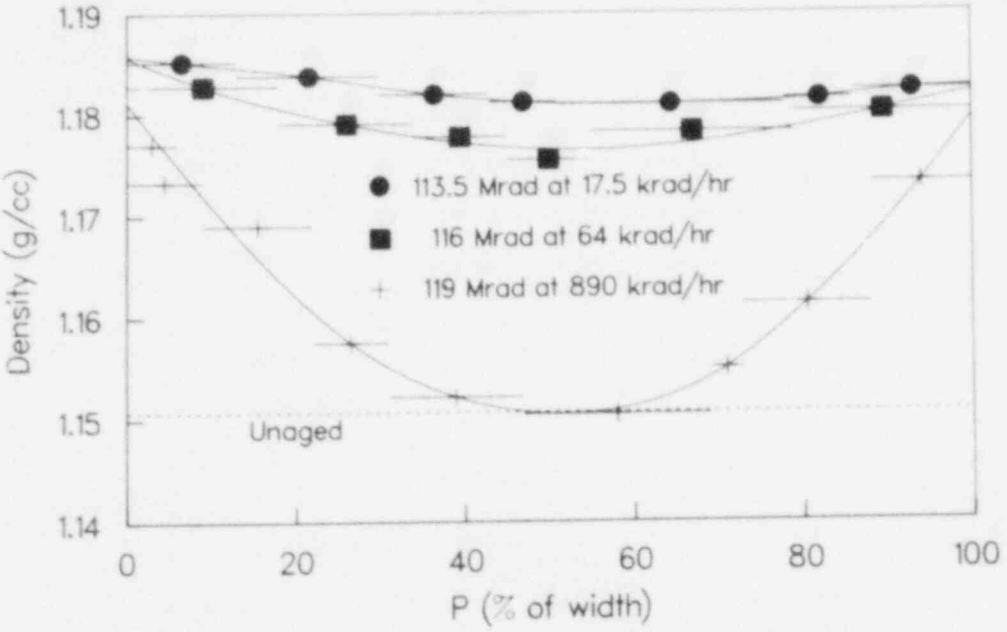


Figure 6: Density profiles for an unaged sample of the chemically crosslinked polyethylene material and for three samples radiation-aged in air to approximately the same total dose but at the three indicated dose rates. The percentage of the distance from the outside to the inside of the sample, P, is plotted as the abscissa. For this material, this distance averaged approximately 0.8 mm.

CLPE and samples radiation aged in air to approximately 115 Mrad at the three indicated dose rates. A straight horizontal line is drawn for the unaged material since the variation in density across unaged samples was found to be less than $\pm$0.001 g/cc. For the aged samples, the density data for the series of slices taken across the sample is plotted as a series of horizontal bars. Each bar spans the region from which the slice was taken, measured as a percentage of the distance from the outside to the inside of the insulation. For this material, this distance averaged approximately 0.8 mm. Under the high dose-rate aging conditions, the oxidation is extremely heterogeneous with substantial oxidation near both the outside and inside surfaces (both of which were air exposed) and essentially no oxidation in the middle of the sample. As the dose rate is lowered, the amount of heterogeneity decreases, with the result that at 17.5 krad/h, the oxidation of the sample is relatively constant across the cross section. These results offer unambiguous evidence that diffusion-limited oxidation is responsible for the dose-rate effects observed in the mechanical property data.

In addition to supplying useful information on physical diffusion processes, density profiles can be valuable for recognizing and understanding chemical dose-rate-effect processes. For instance,

the CLPE profile data of Figure 6 suggests, that at the sample surfaces, the density increase due to oxidation is approximately independent of dose rate. Since diffusion-limited effects are absent at the surfaces, this implies that chemical dose-rate effects are minimal for this material over the range of dose-rate conditions studied.

We are therefore able to infer from the density results for this CLPE material that the oxidation rate is approximately time independent, that chemical dose-rate effects are unimportant and that physical diffusion effects become negligible below approximately 20 krad/h. This information is extremely valuable for predicting radiation aging effects at low dose rates. Additional information on the kinetics underlying the oxidative degradation is available from detailed analyses of the profile shapes and their dependencies on dose rate. This topic will be discussed in a forthcoming publication.[13]

Our other example for radiation environments concerns a case in which both physical and chemical dose-rate effects are significant. Figure 7 shows normalized tensile elongation data for the low density polyethylene (PE) material plotted against total radiation dose. The material was aged in air at 43°C at the three indicated dose rates. In contrast to the CLPE, the dose-rate effects for this material are substantial and give no indication of disappearing at low dose rates. Density profiles were obtained for badly degraded samples ($e/e_0 \sim 0.1$) at each of the three dose rates and for an unaged sample. The unaged material had a flat profile with density equal to a constant 0.925 g/cc. As usual, the density of the oxidized materials increased with respect to the unaged density. For convenience of presentation, the observed changes in density for the aged samples were divided by the appropriate radiation dose (114, 23, and 11 Mrad respectively at 946, 20, and 3 krad/h). The resulting profiles in Figure 8 therefore give the change in density per Mrad, plotted across the sample. These density profiles show that oxygen-diffusion-limited degradation is very important at the highest dose rates but becomes insignificant at the lowest.

Figure 9 shows the density at the outer edge of the polyethylene samples plotted versus dose at the three indicated dose rates. For a constant total dose, the change in edge density increases by a factor of ~6 in going from 946 krad/h to 3 krad/h. Since the edge density is unaffected by diffusion effects, these results indicate that chemical dose-rate mechanisms are partly responsible for the mechanical property dose-rate effects. Easily recognizing the conditions under which the physical diffusion mechanism disappears, and readily determining when such chemical effects exist, underscore two of the reasons for the utility of density profiling.

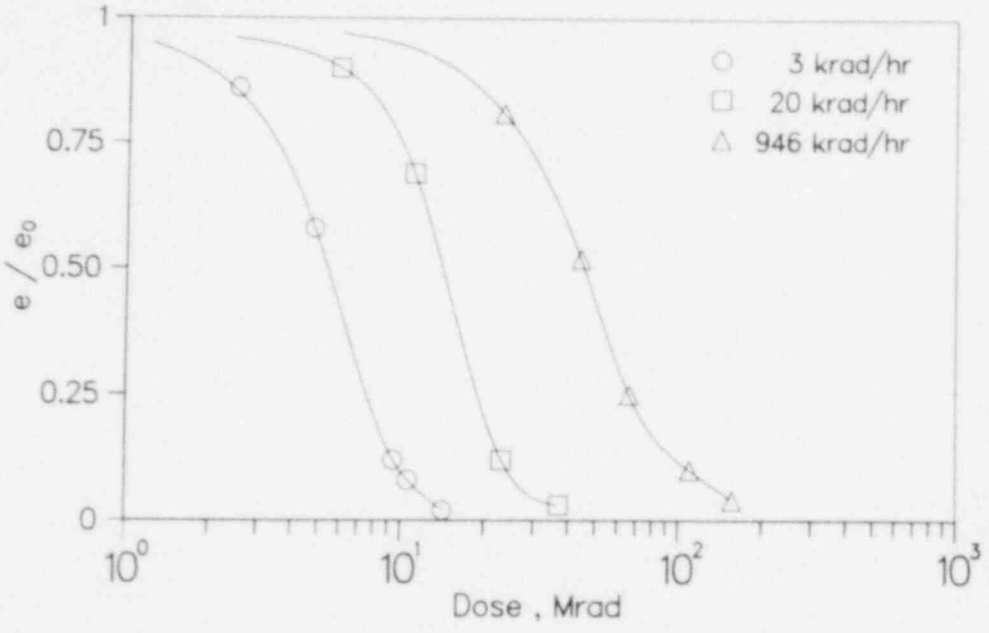


Figure 7: Normalized tensile elongation data versus radiation dose for a low density polyethylene material which had been aged in air at 43°C at the three indicated dose rates.

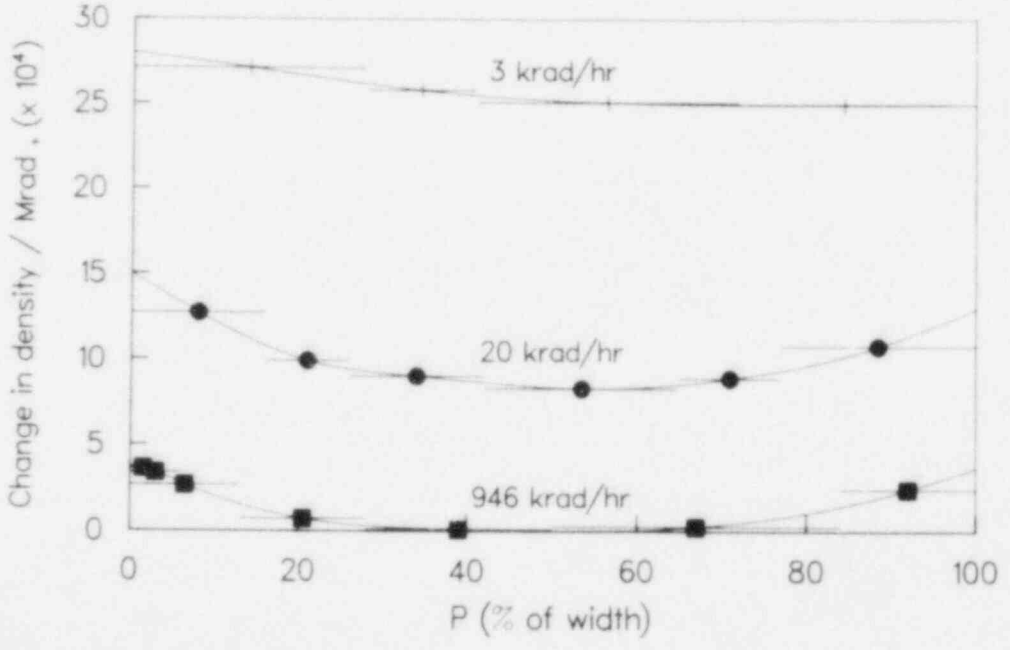


Figure 8: Profiles of the change in density per Mrad of radiation dose for three samples of the low density polyethylene material, which were aged in air at the three indicated dose rates. P represents the percentage of the distance from the outside edge to the inside edge of the sample. This distance averaged approximately 0.8 mm for this material.

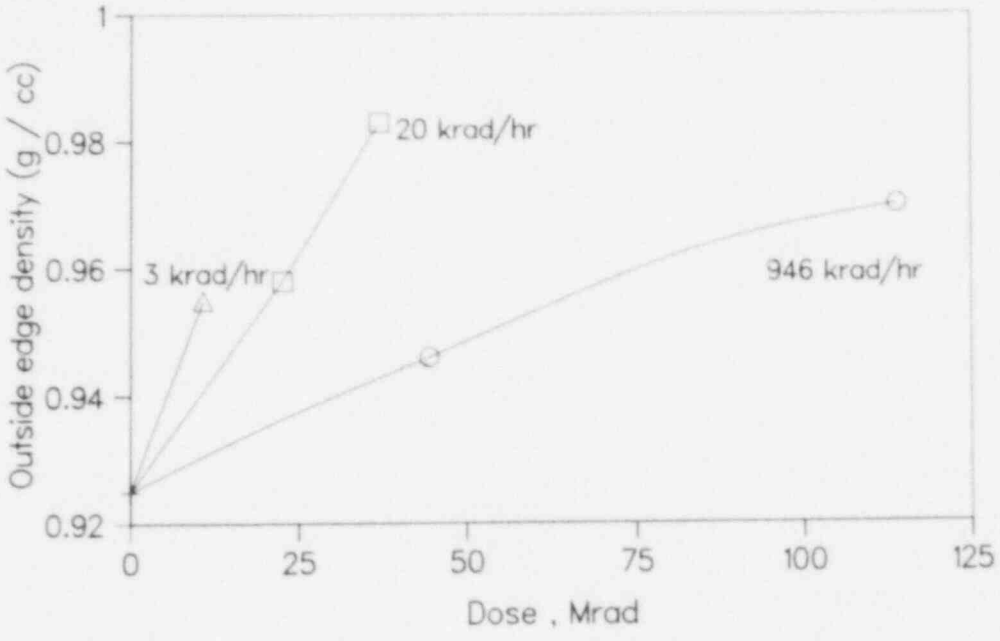


Figure 9: Density at the outer edge of the polyethylene insulation material plotted versus radiation dose at the three indicated dose rates.

When chemical as well as physical dose-rate mechanisms are important for a material, radiation-aging simulations can be quite difficult. Density and other profiling techniques will sometimes allow one to experimentally eliminate the heterogeneous, diffusion-dominated aging environments and thus concentrate on the environments dominated by homogeneous chemical effects. This approach was successfully implemented on a PVC material which had a very complex aging behavior caused by physical (diffusion-limited) and chemical (hydroperoxide-breakdown) effects [6]. A general kinetic model for the hydroperoxide-mediated dose-rate effect was derived and successfully applied to the homogeneous-aging regions. The resulting extrapolated predictions were in excellent agreement with 12-year real-time nuclear power plant aging results [6]. This same chemical dose-rate mechanism is a major contributor [14] to the chemical dose-rate effects of polyethylene shown in Figure 9.

The above results suggest a generalized approach for aging simulations in radiation environments. It involves the use of profiling techniques both to learn the importance of the physical dose-rate mechanism (oxygen diffusion-limited effects) and to determine how low a dose rate is necessary to eliminate these effects. If chemical dose-rate effects are unimportant, aging simulations can be carried out by going to dose rates low enough

to eliminate the physical mechanism, followed by the use of the equal-dose, equal-damage assumption. When chemical dose-rate effects are identified, two viable approaches are possible. The material or component can be modified by changing material formulations to eliminate the chemical mechanism or a second material without chemical dose-rate effects can be substituted. Alternatively, in analogy with the hydroperoxide breakdown modelling described above, the chemical dose-rate mechanism can be modelled sufficiently to calculate conditions necessary to simulate ambient aging.

Representative Results for Heat-Aged Materials

The Arrhenius methodology for simulating thermal-aging effects has been extensively applied to materials and components for many years, with reasonable success. Because of this, it has become the most commonly accepted method for simulating lifetimes. It involves the monitoring of material properties at a number of aging temperatures higher than the application temperature, and plotting the log of the time to reach a specified amount of degradation versus the inverse absolute temperature. If a linear plot is found, the Arrhenius activation energy is extracted from the slope and used to select accelerated aging conditions equivalent to application conditions.

Non-Arrhenius behavior can occur for a number of reasons, for example: [7]

1) the existence of two or more important reactions which have differing activation energies, and

2) the presence of diffusion-limited oxidation effects.

Given the limited data often used to derive Arrhenius activation energies, these same mechanisms may be significant yet go experimentally unnoticed. Thus, having simple, sensitive techniques capable of recognizing the presence of such mechanisms will substantially increase confidence levels when applying the Arrhenius approach. Density profiling is one technique capable of achieving such a goal.

In typical elevated-temperature environments, the mechanisms leading to density increases are slightly different from those discussed earlier for moderate to low temperature radiation exposures. Normally, the weight of gaseous products released during oxidation will be larger than the weight of covalently bonded oxygen added to the material. Thus, both the sample weight and volume will decrease; since the volume decrease is usually faster, the density will tend to increase. In filled polymers, these increases will be much larger since weight loss of polymer will

lead to an increase in the weight fraction of the higher density filler material (e.g., clay).

Figure 10 shows density profiles for air-oven aged nitrile rubber samples of thickness ~1.5 mm. The results in Figure 10A show an unaged profile and profiles for 2 day and 7 day exposures at 150°C. These conditions represent moderate and severe mechanical degradation, with the ultimate tensile elongation dropping to ~60% and 5% of the initial value, respectively. The unaged profile is not quite flat, probably due to slight thermal gradients during compression-molding of the slabs used in the study. The profiles for the aged materials indicate that important oxygen-diffusion effects exist for both aging times at 150°C, with very little oxidation occurring near the centers of the samples. The results in Figure 10B show profiles taken for samples aged for 7 days and 28 days at 130°C, again corresponding to moderate and severe mechanical degradation respectively. Diffusion effects for the severely degraded sample are significant but appear to be reduced compared to the 7 day result at 150°C. This is as anticipated since diffusion activation energies are normally lower than the activation energies for thermal oxidation. In contrast, the results for the moderately degraded sample at 130°C appear to indicate that diffusion effects are less important at earlier times. These results are consistent with a degradation rate that increases with aging time. In other words, at earlier times, diffusion processes are capable of supplying sufficient oxygen to the sample interior, whereas at later stages in the degradation, the rate of oxygen consumption increases (and/or the diffusion rate

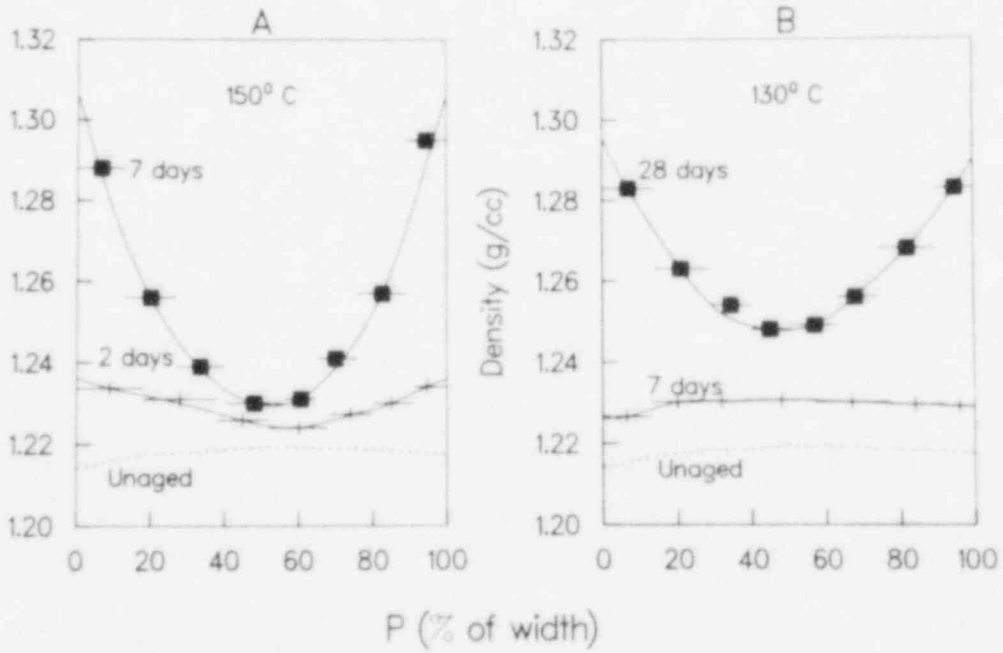


Figure 10: Density profiles for the nitrile rubber material heat aged in air. A: aging at 150°C. B: aging at 130°C.

of oxygen decreases) until this is no longer true. This result is in accord with the frequently observed phenomenon that thermal-oxidative degradation of many organic materials exhibits an induction period. That is, the oxidation of a material starts out slowly, but accelerates as time goes on.

When oxygen-diffusion effects lead to heterogeneously degraded samples, comparisons of material degradation parameters (e.g., mechanical property data) obtained at different temperatures must be viewed with suspicion. If extrapolations of elevated temperature data are attempted, diffusion effects need to be eliminated. One way of accomplishing this is to lower the exposure temperatures until homogeneously aged samples are confirmed.

Even when the experimental conditions eliminate diffusion effects, density profiling will often give other useful information. An example involves the EPR cable insulation material. Oven aging results for this material, covering a temperature range of 100°C to 170°C, give non-Arrhenius behavior at both high and low temperatures, as shown in Figure 11. It is interesting to note that this non-Arrhenius character evidences itself by a slow, subtle change in activation energy, occurring over a fairly large temperature range. More limited temperature studies covering a smaller temperature range would have probably concluded that Arrhenius behavior was found. At the higher temperatures, some contribution from diffusion effects might be expected. However, given the relatively high oxygen permeation rate for EPR materials [15] coupled with the very long aging times, diffusion effects under the lower temperature aging conditions were not anticipated. This was confirmed by density profiling, but a second heterogeneous effect was observed. Figure 12 shows density profiles for samples aged at the lowest aging temperature and for an unaged sample. Very little change occurs with aging except near the inside surface of the insulation where dramatic density increases are noted. This enhanced oxidation near the inside of the insulation is due to catalysis by copper species, a mechanism which has been observed in numerous thermal oxidative studies of polyolefin materials [16-18] and also identified using density profiling in room temperature radiation exposures [4]. Although the EPR insulation samples were stripped from the copper conductors before aging, copper salts could easily have diffused into the insulation during the high-temperature extrusion manufacturing process. Enhanced copper concentrations near the inside surface of the insulation were confirmed using emission spectroscopy and microprobe analysis.

Density profiling results at other temperatures indicate that the copper-catalyzed oxidation mechanism has a higher activation energy than the normal oxidation of this material. This implies that as the temperature is lowered, the former becomes less important [13], explaining the observed upward curvature in the Arrhenius curve.

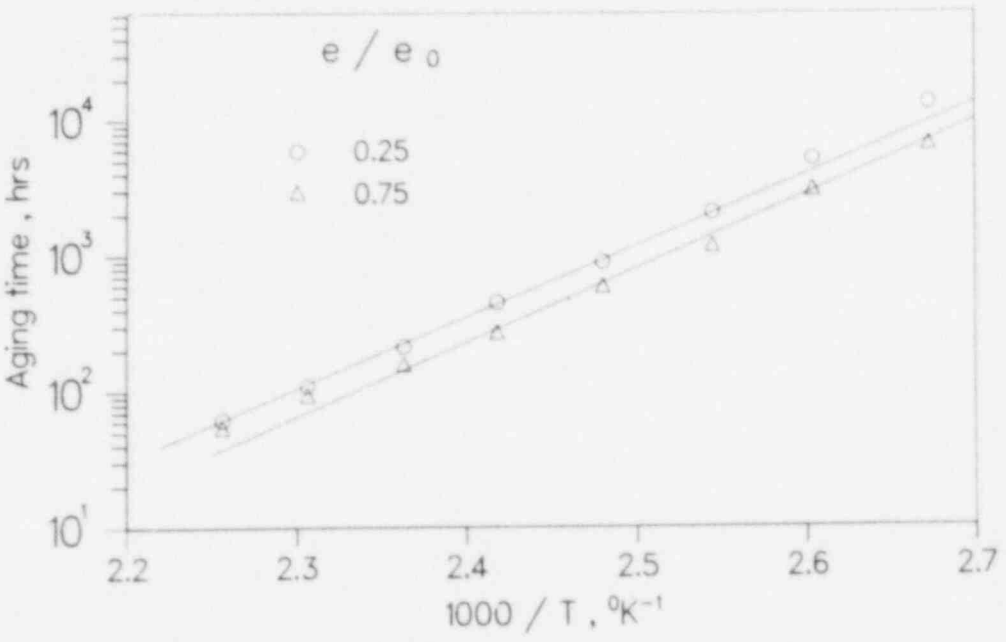


Figure 11: Arrhenius plot of thermal aging data for EPR. The log of the time required for the ultimate tensile elongation to decrease to 75% and 25% of original is plotted versus inverse absolute temperature.

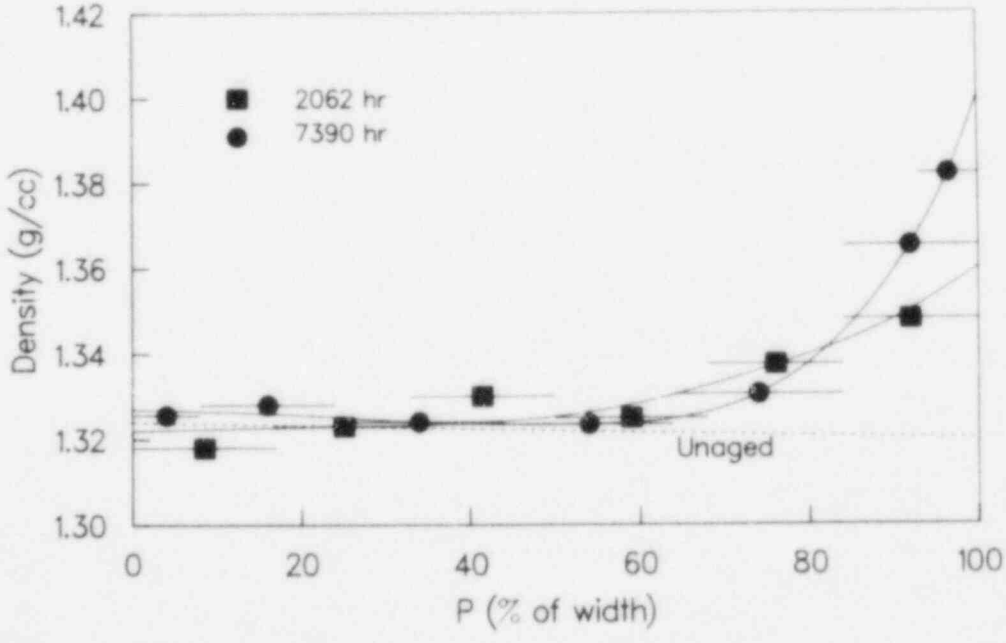


Figure 12: Density profiles for the EPR cable insulation material which had been heat aged in air at 100°C.

The observation that copper-catalyzed oxidation can contribute significantly to the thermal degradation of this EPR material underscores the potential dangers inherent in material degradation studies that overlook possible material interactions. For instance, if thermal aging studies were done on compression-molded sheets of this material, copper-catalyzed oxidation would not be observed.

Another useful aspect to the density profiling technique is that it is often very sensitive to the early stages of degradation. Figure 13 shows mechanical property data versus time for this EPR material at 100°C. Comparing this data to the density profile data of Figure 12 shows that significant changes occur in the density profiles before noticeable changes are apparent in the mechanical properties.

Representative Results for Mechanically-Stressed Samples

Stress-relaxation studies are often used to predict material response for materials which are mechanically stressed, such as seals and gaskets. Again, reliable conclusions can be critically dependent upon eliminating diffusion effects from the accelerated simulations [19]. Density profiling offers a rapid and easy method for determining when such effects are present. Figure 14 shows, for example, a density profile for the ethylene propylene seal material which was aged under 15% tensile strain for 69 hours at 48°C and 850 krad/h. Even though the oxygen permeation rate in EPR materials is relatively high [15], significant diffusion effects occur under the above experimental conditions. Clearly, to have confidence in accelerated aging simulations of mechanically-stressed materials, diffusion effects must first be eliminated. Density profiling techniques can be conveniently used to determine how low a dose rate (and/or temperature) is necessary to eliminate such artifacts.

## CONCLUSIONS

Density profiling is an extremely sensitive, rapid and inexpensive analytical technique for studying polymers. Although it can be applied to unaged materials for determining whether material inhomogeneities exist and thus serve as a means of screening for insufficient component mixing or the possible presence of temperature gradients during cure, its main applications stem from the observation that large density increases can occur in air-aging environments. Since the technique is capable of measuring the density of very thin (less than 25 micrometer) samples, it is ideal for investigating inhomogeneous oxidation mechanisms, such as diffusion-limited oxidation. This mechanism plays an important role in the degradation of numerous materials and can be induced by heat, high-energy radiation, and mechanical stress. For aging

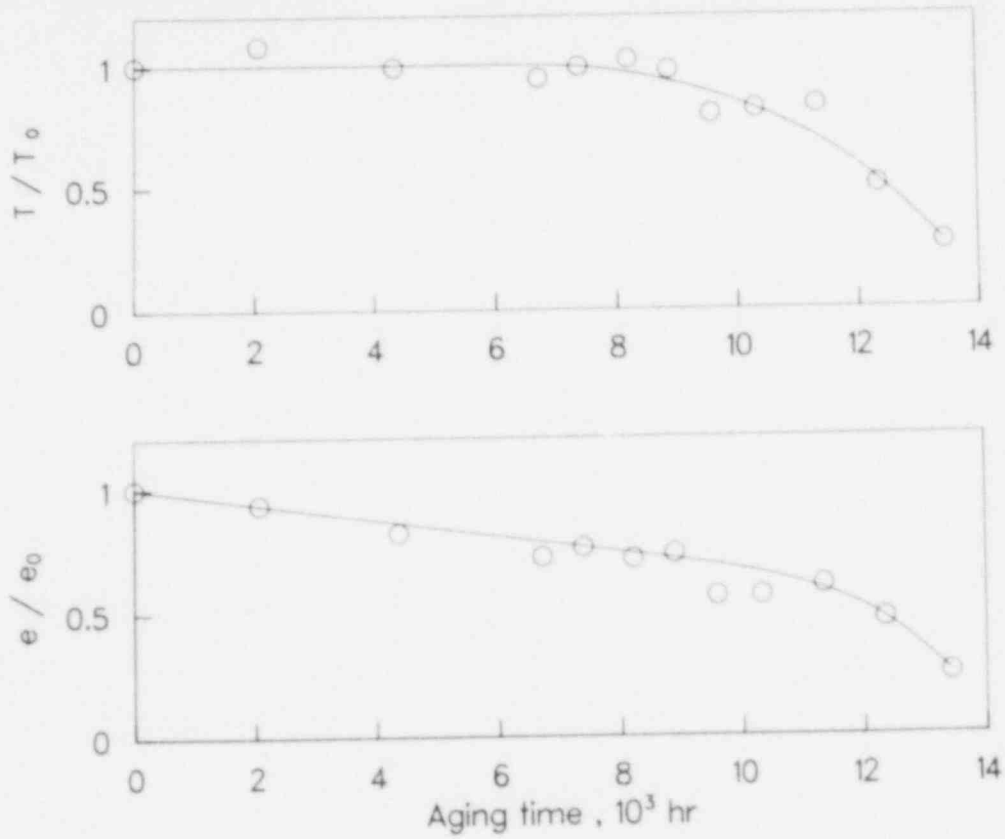


Figure 13: Mechanical property heat aging results at 100°C for the EPR cable insulation material. The tensile strength after aging divided by the tensile strength before aging ($T/T_o$) and the tensile elongation after aging divided by the tensile elongation before aging ($e/e_o$) are plotted against the aging time.

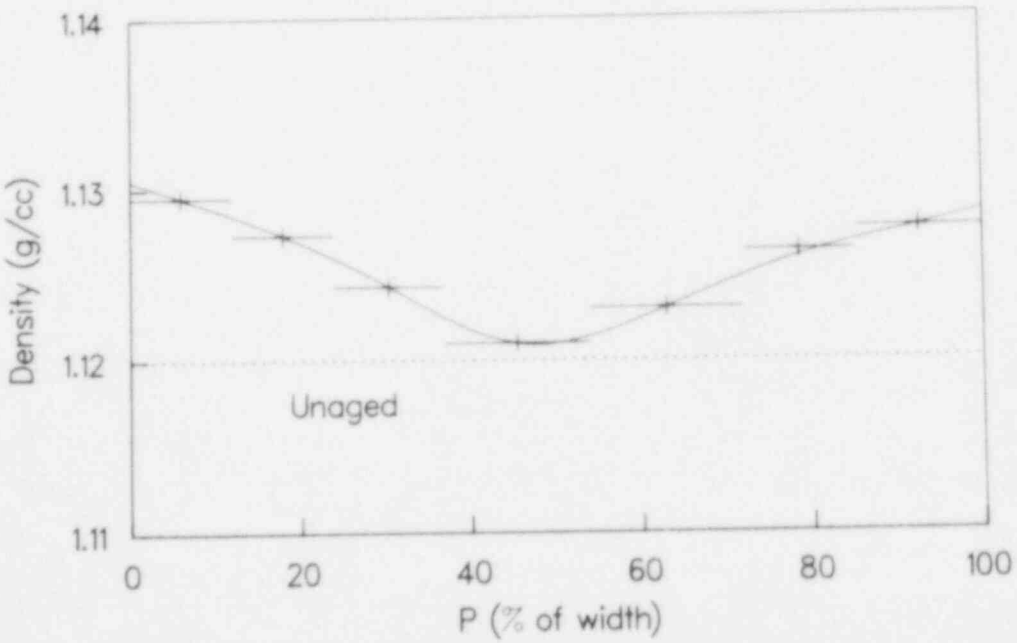


Figure 14: Density profile of an EPR O-ring material after exposure to mechanical tensile stress during radiation aging.

tests involving these environments either singly or in combination, the elimination of diffusion effects is critical to reliable predictions of material response under long-term exposures.

Besides affording an easy method for determining experimental conditions under which diffusion effects are no longer significant, density profiling is also useful for determining and understanding the chemical mechanisms important to oxidation. For instance, density profiling can yield information on whether oxidation reactions are constant with time or have autocatalytic behavior. It is also useful for observing inhomogeneous oxidation effects near material interfaces caused by localized material poisoning or incompatibilities. In high-energy radiation environments, density profiling allows conclusions to be made about the existence of chemical dose-rate effects. The above applications imply that density profiling will be of great utility in the development of methodologies for simulating aging of nuclear power plant components.

## REFERENCES


1. G. J. van Amerongen, Rubber Chem. & Tech. 37, 1065 (1964).

2. H. Matsuo and M. Dole, J. Phys. Chem. 63, 837 (1959).

3. A. V. Cunliffe and A. Davis, Polym. Degr. Stab. 4, 17 (1982).

4. K. T. Gillen and R. L. Clough, Radiat. Phys. Chem. 22, 537 (1983).

5. R. L. Clough, K. T. Gillen and C. A. Quintana, Heterogeneous Oxidative Degradation in Irradiated Polymers, NUREG/CR-3643, SAND83-2493, Sandia National Laboratories, Albuquerque, New Mexico, April 1984. (also published in J. Polym. Sci., P.C. Ed. 23, 359 (1985).

6. K. T. Gillen and R. L. Clough, General Extrapolation Model for an Important Chemical Dose-Rate Effect, NUREG/CR-4008, SAND84-1984, Sandia National Laboratories, Albuquerque, New Mexico, December, 1984. (also J. Polym. Sci., P. C. Ed., in press).

7. K. T. Gillen and K. E. Mead, Predicting Life Expectancy and Simulating Age of Complex Equipment Using Accelerated Aging Techniques, NUREG/CR-1466, SAND79-1561, Sandia National Laboratories, Albuquerque, New Mexico, January 1980.

8. T. N. Bowmer, L. K. Cowen, J. H. O'Donnel and D. J. Winzor, J. Appl. Polym. Sci. 24, 425 (1979).

9. I. Kuriyama, N. Hayakawa, Y. Nakase, J. Ogura, H. Yagyu and K. Kasai, IEEE Trans. El. Ins. EI-14, 272 (1979).

10. K. T. Gillen, R. L. Clough and L. H. Jones, Investigation of Cable Deterioration in the Containment Building of the Savannah River Nuclear Reactor, NUREG/CR-2877, SAND81-2613, Sandia National Laboratories, Albuquerque, New Mexico, August 1982.

11. D. A. Blackadder and J. S. Keniry, Macromol. Chem. 141, 211(1971).

12. R. K. Sharma and L. Mandelkern, Macromol. 2, 266(1969).

13. K. T. Gillen, unpublished results.

14. R. L. Clough and K. T. Gillen, Radiation-Thermal Degradation of PE and PVC: Mechanism of Synergism and Dose-Rate Effects, NUREG/CR-2156, SAND80-2149, Sandia National Laboratories, Albuquerque, New Mexico, June 1981. (also published in Rad. Phys. and Chem. 18, 661 (1981).

15. T. Seguchi, S. Hashimoto, K. Arakawa, N. Hayakawa, W. Kawakami and I. Kuriyama, Radiat. Phys. Chem. 17, 195 (1981).

16. M. G. Chan and D. L. Allara, J. Colloid Interface Sci., 47, 697 (1974).

17. M. G. Chan and D. A. Allara, Polym. Eng. Sci., 4, 12 (1974).

18. L. Reich and S. Stivala, Elements of Polymer Degradation, McGraw-Hill, New York (1971).

19. K. Ono, A. Kaeriyama and K. Murakami, J. Polym. Sci., P.C. 13, 2615 (1975).

DISTRIBUTION:

U.S. Government Printing Office
Receiving Branch (Attn: NRC Stock)
8610 Cherry Lane
Laurel, MD 20707
375 copies for RV

Ansaldo Impianti
Centro Sperimentale del Boschetto
Corso F.M. Perrone, 118
16161 Genova
ITALY
Attn: C. Bozzolo

Ansaldo Impianti
Via Gabriele D'Annunzio, 113
16121 Genova
ITALY
Attn: S. Grifoni

ASEA-ATOM
Department KRD
Box 53
S-721 04
Vasteras
SWEDEN
Attn: A. Kjellberg

ASEA-ATOM
Department TQD
Box 53
S-721 04
Vasteras
SWEDEN
Attn: T. Granberg

ASEA KABEL AB
P.O. Box 42 108
S-126 12
Stockholm
SWEDEN
Attn: B. Dellby

Atomic Energy of Canada, Ltd.
Chalk River Nuclear Laboratories
Chalk River, Ontario K0J 1J0
CANADA
Attn: G. F. Lynch

Atomic Energy of Canada, Ltd.
1600 Dorchester Boulevard West
Montreal, Quebec H3H 1P9
CANADA
Attn: S. Nish

Atomic Energy Research Establishment
Building 47, Division M.D.D.
Harwell, Oxfordshire
OX11 ORA,
ENGLAND
Attn: S. G. Burnay

Bhabha Atomic Research Centre
Health Physics Division
BARC
Bombay-85
INDIA
Attn: S. K. Mehta

British Nuclear Fuels Ltd.
Springfields Works
Salwick, Preston
Lancs
ENGLAND
Attn: W. G. Cunliff, Bldg 334

Brown Boveri Reaktor GMBH
Postfach 5143
D-6800 Mannheim 1
WEST GERMANY
Attn: R. Schemmel

Bundesanstalt fur Materialprufung
Unter den Eichen 87
D-1000 Berlin 45
WEST GERMANY
Attn: K. Wundrich

CEA/CEN-FAR
Departement de Surete Nucleaire
Service d'Analyse Fonctionnelle
B.P. 6
92260 Fontenay-aux-Roses
FRANCE
Attn: M. Le Meur
J. Henry

CERN
Laboratorie 1
CH-1211 Geneve 23
SWITZERLAND
Attn: H. Schonbacher

Canada Wire and Cable Limited
Power & Control Products Division
22 Commercial Road
Toronto, Ontario
CANADA M4G 1Z4
Attn: Z. S. Paniri

Centro Elettrotecnico
Sperimentale Italiano
Research and Development
Via Rubattino 54
20134 Milan,
ITALY
Attn: Carlo Masetti

Commissariat a l'Energie Atomique
ORIS/LABRA
BP N° 21
91190 Gif-Sur-Yvette
FRANCE
Attn: G. Caussens
J. Chenion
F. Carlin

Commissariat a l'Energie Atomique
CEN Cadarche DRE/STRE
BP N° 1
13115 Saint Paul Lez Durance
FRANCE
Attn: J. Campan

Conductores Monterrey, S. A.
P.O. Box 2039
Monterrey, N. L.
MEXICO
Attn: P. G. Murga

Electricite de France
(S.E.P.T.E.N.)
12, 14 Ave. Dubrieroz
69628 Villeurbarnie
Paris, FRANCE
Attn: H. Herouard
M. Hermant

Electricite de France
Direction des Etudes et Recherches
1, Avenue du General de Gaulle
92141 CLAMART CEDEX
FRANCE
Attn: J. Roubault
L. Deschamps

Electricite de France
Direction des Etudes et Recherches
Les Renardieres
Boite Postale n° 1
77250 MORET SUR LORING
FRANCE
Attn: Ph. Roussarie
V. Deglon
J. Ribot

EURATOM
Commission of European Communities
C.E.C. J.R.C.
21020 Ispra (Varese)
ITALY
Attn: G. Mancini

FRAMATOME
Tour Fiat - Cedex 16
92084 Paris La Defense
FRANCE
Attn: G. Chauvin
E. Raimondo

Furukawa Electric Co., Ltd.
Hiratsuka Wire Works
1-9 Higashi Yawata - 5 Chome
Hiratsuka, Kanagawa Pref
JAPAN 254
Attn: E. Oda

Gesellschaft fur Reaktorsicherheit (GRS) mbH
Glockengasse 2
D-5000 Koln 1
WEST GERMANY
Attn: Library

Health & Safety Executive
Thames House North
Milbank
London SW1P 4QJ
ENGLAND
Attn: W. W. Ascroft-Hutton

ITT Cannon Electric Canada
Four Cannon Court
Whitby, Ontario L1N 5V8
CANADA
Attn: B. D. Vallillee

Imatran Voima Oy
Electrotechn. Department
P.O. Box 138
SF-00101 Helsinki 10
FINLAND
Attn: B. Regnell
K. Koskinen

Institute of Radiation Protection
Department of Reactor Safety
P.O. Box 268
00101 Helsinki 10
FINLAND
Attn: L. Reiman

Instituto de Desarrollo y Diseno
Ingar - Santa Fe
Avellaneda 3657
C.C. 34B
3000 Santa Fe
REPUBLICA ARGENTINA
Attn: N. Labath

Japan Atomic Energy Research Institute
Takasaki Radiation Chemistry
Research Establishment
Watanuki-machi
Takasaki, Gunma-ken
JAPAN
Attn: N. Tamura
K. Yoshida
T. Seguchi

Japan Atomic Energy Research Institute
Tokai-Mura
Naka-Gun
Ibaraki-Ken
319-11
JAPAN
Attn: Y. Koizumi

Japan Atomic Energy Research Institute
Osaka Laboratory for Radiation Chemistry
25-1 Mii-Minami machi,
Neyagawa-shi
Osaka 572
JAPAN
Attn: Y. Nakase

Kalle Niederlassung der Hoechst AG
Postfach 3540
6200 Wiesbaden 1,
WEST GERMANY
Biebrich
Attn: Dr. H. Wilski

Kraftwerk Union AG
Department R361
Hammerbacherstrasse 12 + 14
D-8524 Erlangen
WEST GERMANY
Attn: I. Terry

Kraftwerk Union AG
Section R541
Postfach: 1240
D-8757 Karlstein
WEST GERMANY
Attn: W. Siegler

Kraftwerk Union AG
Hammerbacherstrasse 12 + 14
Postfach: 3220
D-8520 Erlangen
WEST GERMANY
Attn: W. Morell

Motor Columbus
Parkstrasse 27
CH-5401
Baden
SWITZERLAND
Attn: H. Fuchs

National Nuclear Corporation
Cambridge Road
Whetstone
Leicester LE8 3LH
ENGLAND
Attn: A. D. Hayward
J. V. Tindale

NOK AG Baden
Beznau Nuclear Power Plant
CH-5312 Doettingen
SWITZERLAND
Attn: O. Tatti

Norsk Kabelfabrik
3000 Drammen
NORWAY
Attn: C. T. Jacobsen

Nuclear Power Engineering Test Center
6-2, Toranomon, 3-Chome
Minato-ku
No. 2 Akiyana Building
Tokyo 105
JAPAN
Attn: K. Takumi

Ontario Hydro
700 University Avenue
Toronto, Ontario M5G 1X6
CANADA
Attn: R. Wong
B. Kukreti

Oy Stromberg Ab
Helsinki Works
Box 118
FI-00101 Helsinki 10
FINLAND
Attn: P. Paloniemi

Radiation Center of
Osaka Prefecture
Radiation Application-
Physics Division
Shinke-Cho, Sakai
Osaka, 593, JAPAN
Attn: S. Okamoto

Rappinl
ENEA-PEC
Via Arcoveggio 56/23
Bologna
ITALY
Attn: Ing. Ruggero

Rheinisch-Westfallscher
Technischer Uberwachunge-Vereln e.V.
Postfach 10 32 61
D-4300 Essen 1
WEST GERMANY
Attn: R. Sartori

Sydkraft
Southern Sweden Power Supply
21701 Malmo
SWEDEN
Attn: O. Grondalen

Technical University Munich
Institut for Radiochemie
D-8046 Garching
WEST GERMANY
Attn: Dr. H. Heusinger

UKAEA
Materials Development Division
Building 47
AERE Harwell
OXON OX11 ORA
ENGLAND
Attn: D. C. Phillips

United Kingdom Atomic Energy Authority
Safety & Reliability Directorate
Wigshaw Lane
Culcheth
Warrington WA3 4NE
ENGLAND
Attn: M. A. H. G. Alderson

Waseda University
Department of Electrical Engineering
4-1 Ohkubo-3, Shinjuku-ku
Tokyo
JAPAN
Attn: K. Yahagi

1200 J. P. VanDevender
1800 R. L. Schwoebel
1810 R. G. Kepler
1811 R. L. Clough (5)
1812 L. A. Harrah
1812 K. T. Gillen (5)
1812 N. J. Dhooge
1813 J. G. Curro
2155 J. E. Gover
2155 O. M. Stuetzer
6200 V. L. Dugan
6300 R. W. Lynch
6400 A. W. Snyder
6410 J. W. Hickman
6417 D. D. Carlson
6420 J. V. Walker
6433 F. V. Thome
6440 D. A. Dahlgren
6442 W. A. Von Riesemann
6444 L. D. Buxton
6446 L. L. Bonzon (10)
6446 W. H. Buckalew
6446 L. D. Bustard
6446 J. W. Grossman
6446 J. D. Keck
6446 E. H. Richards
6446 F. J. Wyant
6447 D. L. Berry
6447 P. R. Bennett
6449 K. D. Bergeron
6450 J. A. Reuscher
8024 M. A. Pound
3141 C. M. Ostrander (5)
3151 W. L. Garner

NRC FORM 336 (12-84) NRCM 1102, 3201, 3202

U.S. NUCLEAR REGULATORY COMMISSION

**BIBLIOGRAPHIC DATA SHEET**

SEE INSTRUCTIONS ON THE REVERSE

1 REPORT NUMBER (Assigned by TIDC and Vol. No. if any)

NUREG/CR-4356
SAND85-1557

2 TITLE AND SUBTITLE

Applications of Density Profiling to Equipment Qualification Issues

3 LEAVE BLANK

4 DATE REPORT COMPLETED

MONTH: July — YEAR: 1985

5 AUTHOR(S)

K. T. Gillen, R. L. Clough and N. J. Dhooge

6 DATE REPORT ISSUED

MONTH: September — YEAR: 1985

7 PERFORMING ORGANIZATION NAME AND MAILING ADDRESS (Include Zip Code)

Sandia National Laboratories
Albuquerque, New Mexico 87185

8 PROJECT/TASK/WORK UNIT NUMBER

9 FIN OR GRANT NUMBER

A-1051

10 SPONSORING ORGANIZATION NAME AND MAILING ADDRESS (Include Zip Code)

Electrical Engineering Instrumentation and Control Branch
Division of Engineering Technology
Office of Nuclear Regulatory Research
U.S. Nuclear Regulatory Commission
Washington, DC 20555

11a TYPE OF REPORT

b PERIOD COVERED (Inclusive dates)

12 SUPPLEMENTARY NOTES

13 ABSTRACT (200 words or less)

This paper reviews the density profiling technique, a new, inexpensive and versatile analytical method which can yield extremely useful information on heterogeneities in polymers. The technique makes use of a density gradient column to measure the density of a series of successively-cut slices across a sample. Since the density of very thin slices can easily be obtained, density profiles across very small cross-sections (<1mm) are readily available. A major application of the technique involves oxidation studies of polymers, since oxidation reactions usually lead to substantial increases in polymer density.

Diffusion-limited oxidation effects, which lead to heterogeneously oxidized materials, are often present in polymer aging studies in air. Since these effects are responsible for the commonly-observed physical dose-rate effects in radiation aging environments and for non-Arrhenius behavior in thermal aging environments, the availability of simple oxidation profiling techniques is a tremendous aid in validating the aging simulation aspects of equipment qualification procedures. This paper gives examples of the utility of density profiling for studying oxygen diffusion-limited degradation in both radiation and thermal aging environments and in discovering/understanding chemical dose-rate effects in high energy radiation environments.

14 DOCUMENT ANALYSIS - a KEYWORDS/DESCRIPTORS

b IDENTIFIERS/OPEN-ENDED TERMS

15 AVAILABILITY STATEMENT

GPO Sales
NTIS

16 SECURITY CLASSIFICATION

(This page) Unclass.

(This report) Unclass.

17 NUMBER OF PAGES

18 PRICE